

Entrainment Behavior of Copper and Copper Matte in Copper Smelting Operations

S.W. IP and J.M. TOGURI

In copper smelting, the loss of copper to the slag due to entrainment is largely influenced by the flotation of copper metal and/or matte in the slag phase. To evaluate this behavior, the surface tension of copper as a function of temperature and oxygen pressure and the interfacial tension of the copper-iron matte-slag system as a function of matte grade were measured. From the surface and interfacial tension values, the spreading and flotation coefficients of the copper, matte, and slag system were calculated. Ternary interfacial energy diagrams were also constructed using these data. It is shown that matte droplets containing higher than 32 mass pct Cu will not form a film on rising gas bubbles when they collide in the slag phase. However, matte droplets will attach to gas bubbles upon collision and thus can be floated over the entire range of matte composition. Spreading of copper on bubbles is not possible at oxygen pressures between 10^{-12} and 10^{-8} atm. Flotation of copper by gas bubble in slag is possible at oxygen pressure higher than 10^{-9} atm. However, it is feasible for rising matte droplets (attached to rising bubble) to trap and float copper irrespective of the matte grade.

I. INTRODUCTION

MECHANICALLY entrained matte or metal droplets in slag originate from a variety of sources such as

- (1) converter slag returned to the smelting furnace;
- (2) solid or liquid sulfide from the furnace charge, sliding from unsubmerged regions of the furnace onto the slag and forming a fine dispersion on the slag surface;
- (3) precipitation of copper from slag due to temperature gradients within the furnace;
- (4) sulfur dioxide gas produced in the matte phase dispersing the matte into the slag as the gas crosses the matte-slag interface; and
- (5) attachment of matte or metal droplets to solid magnetite particles present in the slag phase which hinder their settling.

The particular interest of this study is the mechanism of droplet entrainment which results from rising gas bubbles. Depending on the operating conditions, gas bubbles entering the slag phase may float the dispersed droplets away from the matte-slag interface. The ability of gas bubbles to pick up matte droplets is governed by the surface and interfacial tension of the copper, matte, and slag system. Figure 1 shows the three different possible situations that may develop. Minto and Davenport^[1] suggested that case a will occur only if the spreading coefficient as defined by Harkins^[2] is positive. The spreading coefficient is defined as

$$\phi = \gamma_{s/g} - \gamma_{m/g} - \gamma_{m/s} \quad [1]$$

where $\gamma_{s/g}$ = slag surface tension;
 $\gamma_{m/g}$ = matte surface tension; and
 $\gamma_{m/s}$ = matte-slag interfacial tension.

Flotation of droplets by gas bubbles (case b) will occur

if the flotation coefficient is greater than zero. The flotation coefficient is defined as

$$\Delta = \gamma_{s/g} - \gamma_{m/g} + \gamma_{m/s} \quad [2]$$

Case c will take place only if the flotation coefficient is less than zero. Conochie and Robertson^[3] developed a ternary interfacial energy diagram for the prediction of the flotation behavior of the entrained phase. Their approach differs from that of Minto and Davenport^[1] and is based on the balance of surface and interfacial tension forces acting on a droplet resting on a fluid-fluid interface such as the one shown in Figure 2. From such consideration, they obtained the following equations:

$$\gamma_{s/g} = \gamma_{m/g} \cos \theta + \gamma_{m/s} \cos \varphi \quad [3a]$$

Thus,

$$1 - X - Y = Y \cos \theta + X \cos \varphi \quad [3b]$$

$$\gamma_{m/g} \sin \theta = \gamma_{m/s} \sin \varphi \quad [4a]$$

Thus,

$$Y \sin \theta = X \sin \varphi \quad [4b]$$

when

$$X = \frac{\gamma_{m/s}}{\sum \gamma} \quad [5]$$

$$Y = \frac{\gamma_{m/g}}{\sum \gamma} \quad [6]$$

$$Z = \frac{\gamma_{s/g}}{\sum \gamma} \quad [7]$$

where

$$\sum \gamma = \gamma_{s/g} + \gamma_{m/g} + \gamma_{m/s} \quad [8]$$

and

$$X + Y + Z = 1 \quad [9]$$

S.W. IP, Graduate Student, and J.M. TOGURI, Professor, are with the Department of Metallurgy and Materials Science, University of Toronto, Toronto, ON M5S 1A4, Canada.

Manuscript submitted May 17, 1991.

Details concerning the construction of the ternary interfacial energy diagram from the above equations can be obtained from Reference 3.

II. EXPERIMENTAL

The sessile drop technique was adopted for surface and interfacial tension measurements. Images of the drops were taken radiographically using the experimental setup shown in Figure 3. Basically, the main units of the apparatus consisted of an X-ray source, a graphite heating element furnace, and an imaging system. Supporting systems include a temperature-controlling circuit and a gas distribution system which was mainly used for maintaining an inert atmosphere inside the furnace. Details of the apparatus have been described elsewhere.^[4]

A. Copper Surface Tension

High-purity copper from both Cominco American, Inc. (Spokane, WA) and Johnson Matthey Limited (Toronto, ON, Canada) (JM) were used for this study. The Cominco copper was 5N grade in the form of pellets, and the JM copper was Puratronic grade in rod form. Analysis of these two coppers is given in Table I. Prior to each experiment, the copper sample was treated by either immersing in a 2N nitric acid for 2 to 5 minutes or hydrogen reduction for 1 to 4 hours at 873 K. The treated copper was placed on a desired substrate and set inside an alumina crucible. The sample assembly was carefully lowered into the reaction tube and the tube tightly sealed (Figure 4). Two different kinds of materials were used as substrates. They included graphite and mullite (a machinable form). A concave depression was machined on the flat surface of the graphite and mullite discs using semispherical alumina grinding stones. The resulting

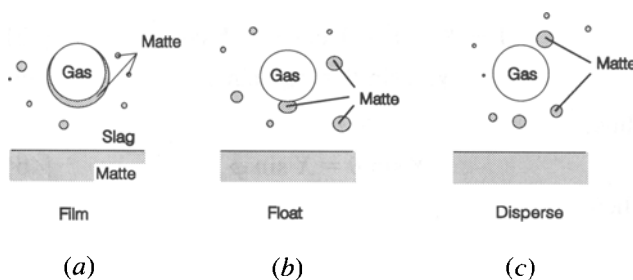


Fig. 1—Interactions between gas bubble and liquid droplets in a continuous phase:^[1] (a) droplet forms a film on the gas bubble, (b) droplet attaches to gas bubble upon contact, and (c) no attachment of droplet to bubble through contact.

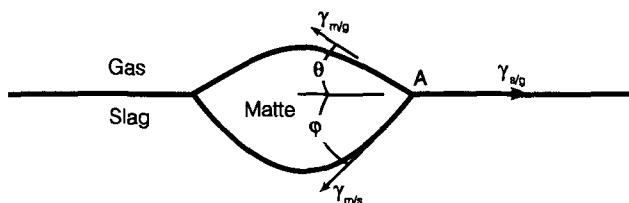


Fig. 2—Diagram illustrating the droplet configuration used in Conochie and Robertson's formulation.^[1]

surface was then polished with 600 or 1000 grit emery paper and fine silicon carbide powder. Each polished substrate was washed ultrasonically in alcohol and stored in a jar of alcohol for later use. Before each experiment, the substrate was cleaned in a 2N HNO₃ solution for 3 to 24 hours and rinsed thoroughly with water.

Gas leakage checks were performed on connections to the experimental system by pressurizing the reaction tube with argon gas. After a gas-tight system was obtained, the reaction tube was evacuated and flushed with argon. The gas chosen for the experiment was then allowed to flow through the reaction tube for one-half to one hour before the sample was heated to the required temperature.

When a symmetric sessile drop was obtained, the drop was allowed to reach thermal equilibrium, about 15 to 30 minutes, before one to three X-ray radiographs were taken. The exposure used was either 70 kV, 150 mA, and 5 to 6 seconds or 100kV, 150 mA, and 0.8 seconds. The film used was a high-resolution KODAK* X-Omat

*KODAK is a trademark of Eastman Kodak Corporation, Rochester, NY.

TL film. This procedure was repeated for each temperature investigated.

The effect of oxygen on the surface tension of copper was examined at 1473 K over an oxygen pressure range of 10⁻¹² to 10⁻⁸ atm. The oxygen pressure was obtained by using appropriate mixtures of CO/CO₂ gas. At any preselected oxygen pressure, the sample was allowed to equilibrate for 1 hour before two radiographs were taken.

To evaluate the surface tension values, the X-ray images on film were converted to their digital equivalent using a computerized image acquisition system which is composed of a Wild M8 stereo microscope, a Cohu 4800 monochrome video camera, a PC VisionPlus frame grabber board, and an ITEX image acquisition software. Coordinate points from the drop profile were extracted from the digital image with a custom-designed digitizing software. These profile points, together with density data, were then fed to a separate computer procedure^[5] to determine the surface tension. Density data for copper were taken from Lucas.^[6] For each sessile drop, three independent sets of profile coordinates were obtained. From these evaluated surface tension values, the observed standard deviation for the data are generally within 0.05 N/m, with a maximum of 0.065 N/m. These high standard deviation values were found to be caused by the use of a rather large size X-ray beam (0.6 mm). The large beam produces a fuzzy edge on the drop image.

B. Matte-Slag Interfacial Tension

The matte used for the experiment was prepared by mixing the required Cu₂S and FeS components. The Cu₂S was obtained from Alpha Chemicals (Ward Hill, MA). The FeS was synthetically prepared from high-purity iron and sulfur, as previously described.^[8] All matte samples were premelted prior to the experiments. Fayalite-type slag was used throughout this study. It was prepared synthetically from an iron, hematite, and silica mixture. Analysis of the slag prior to experiments showed 48.73 pct Fe²⁺, 1.17 pct Fe³⁺, and 36 pct SiO₂, which gives an Fe/SiO₂ ratio of 1.38. The sample arrangement for

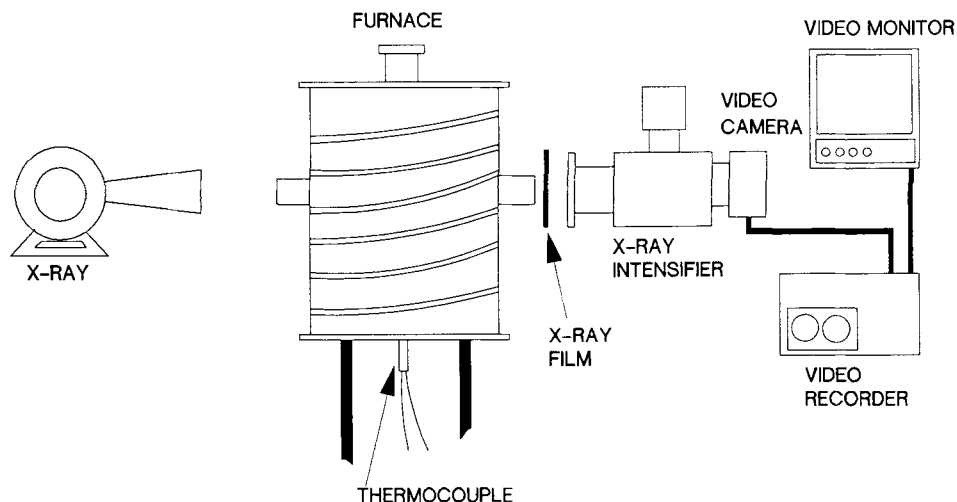


Fig. 3—High-temperature X-ray radiographic apparatus for surface and interfacial tension measurements.

Table I. Chemical Analysis of High-Purity Copper

Element	Cominco*	JM*
Aluminum	<1	<1
Antimony	<0.5	**
Arsenic	<0.5	**
Barium	<4	<1
Beryllium	<0.4	<1
Bismuth	<0.25	<1
Boron	<1	<1
Cadmium	<0.25	<1
Calcium	<2	<1
Chromium	<0.4	<1
Cobalt	<2	<2
Gallium	<0.25	**
Germanium	<4	**
Iron	<4	5
Lead	9	<1
Lithium	**	<1
Magnesium	<0.4	<1
Manganese	0.25	<1
Molybdenum	<0.8	<1
Nickel	<2	<1
Selenium	<0.5	**
Silicon	<5	<1
Silver	2	2
Sodium	8	<1
Tellurium	<0.2	**
Thallium	<0.1	**
Tin	<1	<5
Titanium	<4	**
Vanadium	<4	<1
Zinc	<2	**

*All concentrations are in parts per million.
 **Element not analyzed.

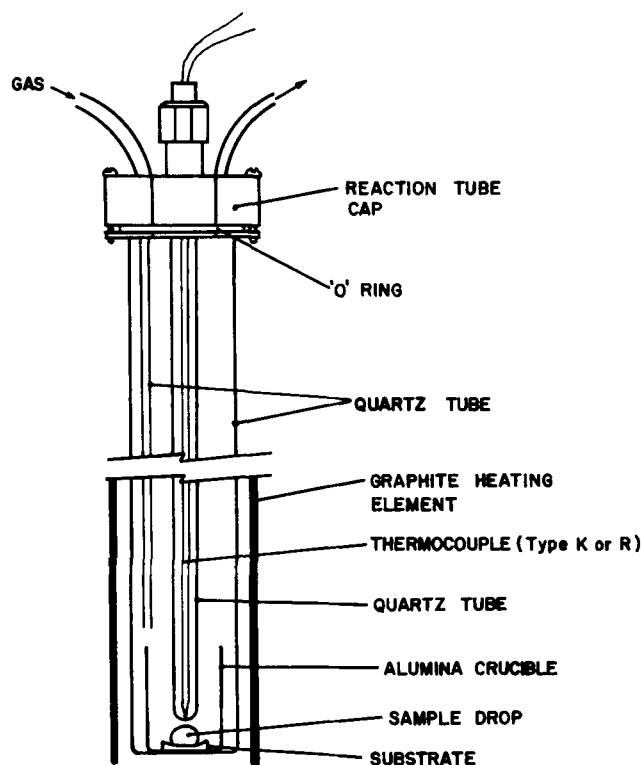


Fig. 4—Experimental setup for surface tension measurements.

the interfacial tension study is shown in Figure 5. Since quartz crucibles were used in all of the experiments, all of the slags involved were silica saturated. The study was carried out at 1473 K under an oxygen-free argon atmosphere.

X-ray radiographs were taken using KODAK X-Omat AR films with an intensifying screen. The exposure used

was 80 kV, 150 mA, and 0.4 to 0.5 seconds for high-grade mattes and 100 kV, 150 mA, and 0.4 to 1.0 seconds for low-grade mattes. Short exposure time was required due to gas evolution from the matte droplets. To obtain the surface and interfacial tension values from the radiographs, the drop image was printed on photographic paper. The drop profiles were then digitized with a digitizing tablet attached to a computer. The digitized points along with density data were input into a recently developed computer procedure^[5] for surface or interfacial tension calculations. The slag density used was 3.6 g/cm³,^[7] and FeS-Cu₂S densities were obtained from the reported values of Kaiura and Toguri.^[8] Similar to

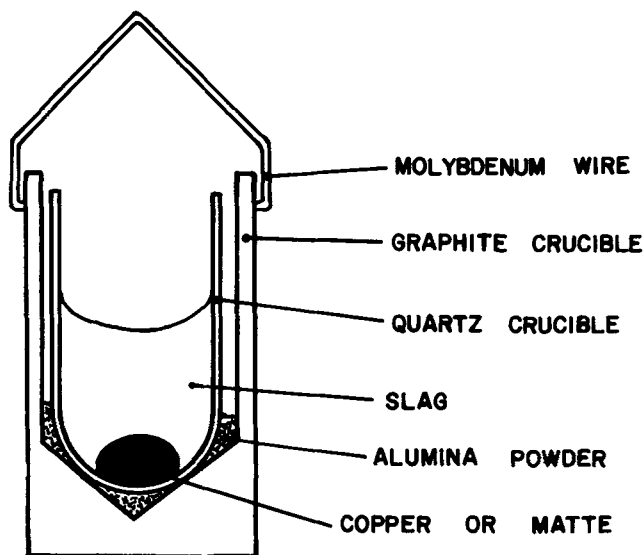


Fig. 5—Sample arrangement for interfacial tension measurements.

the copper surface tension experiments, three sets of independent profile coordinates were obtained from each drop image. The calculated standard deviation changes from a low of 4 pct to a high of 15 pct with decreasing matte grade. The high standard deviation value observed at low matte grade is mainly caused by the poor contrast obtained between the matte and slag on the X-ray image. The poor contrast is attributed to the high amount of iron present in both phases.

III. RESULTS AND DISCUSSION

To establish the reliability of the present experimental technique, the surface tension of a gold sample (Johnson Matthey Specpure grade) was determined. Gold is very inert to surface active elements such as oxygen. Therefore, the measured surface tension will provide a strong

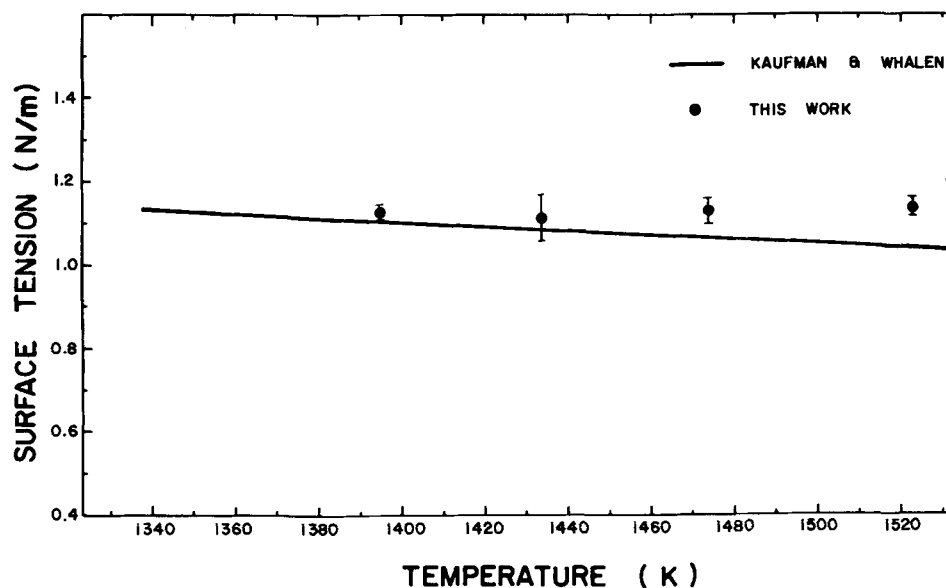


Fig. 6—Surface tension of gold as a function of temperature. Solid line represents result of Kaufman and Whalen.^[10]

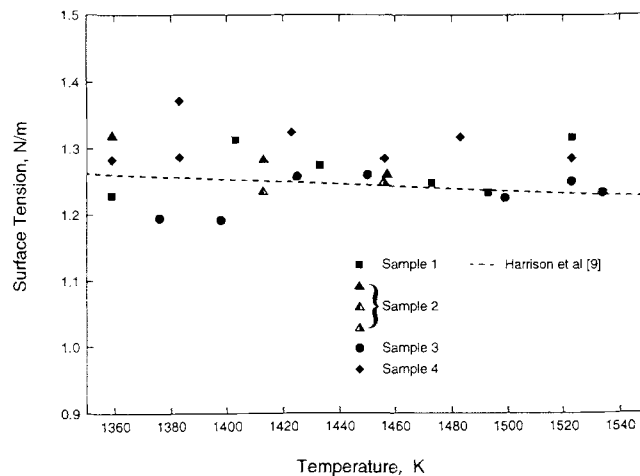


Fig. 7—Surface tension of copper as a function of temperature. The dashed line represents the curve recommended by Harrison *et al.*^[9]

indication as to the reliability of the technique. The measurements were carried out under an argon atmosphere with a mullite substrate. Results of this study are shown in Figure 6. Good agreement was obtained between the present results and those reported by Kaufman and Whalen.^[10]

A number of experiments have been performed on the surface tension of copper in this study. The results are illustrated in Figure 7, along with the recommended values by Harrison *et al.*^[9] based on a review of available data from literature. Experimental conditions corresponding to the different results are given in Table II. As clearly shown in Figure 7, the results obtained from this study are consistent with the curve suggested by Harrison *et al.* To ensure the validity of the results, samples were analyzed before and after each experiment to determine if any pickup of impurities occurred, especially surface active elements, from the substrate or the gas. The results showed that the compositions of the

Table II. Experimental Conditions Used for Copper Surface Tension Measurements

Sample Number	Copper	Substrate	Atmosphere	Comments
1	Cominco	mullite	N ₂ -15 pct H ₂	Copper cleaned with 2N nitric acid; Ti put in crucible as O ₂ getter; hydrogen purified with palladium catalyst.
2	Cominco	graphite	N ₂ -15 pct H ₂ , Ar, Vacuum	Copper treated with hydrogen; (▲) nitrogen-15 pct hydrogen; (△) argon; (△) vacuum.
3	Johnson Matthey	mullite	N ₂ -15 pct H ₂	Copper cleaned with 2N nitric acid.
4	Cominco	mullite	H ₂	Copper treated with hydrogen; Ti in crucible as oxygen getter.

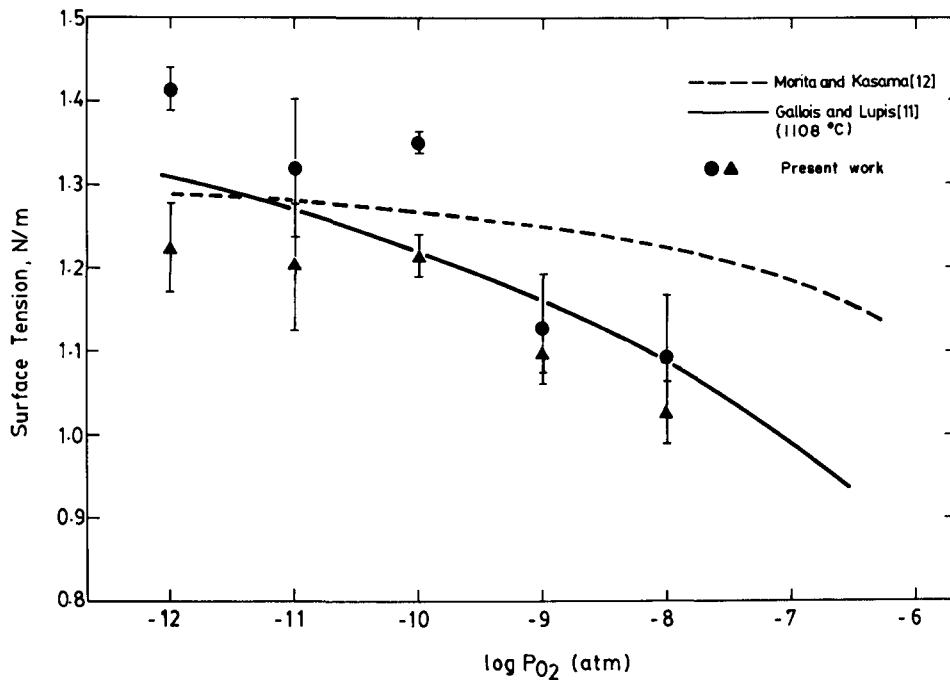


Fig. 8—Surface tension of copper as a function of oxygen pressure at 1473 K.

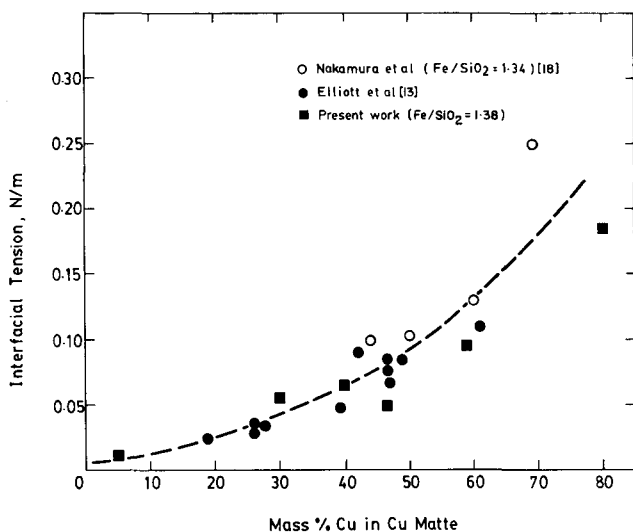


Fig. 9—Interfacial tension of the matte-slag system at 1473 K.

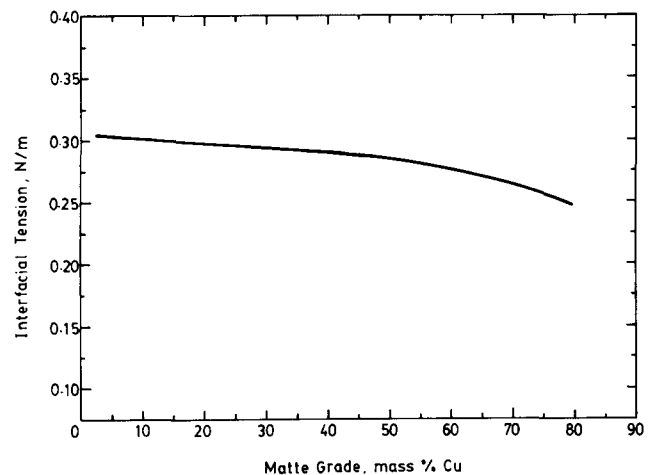


Fig. 10—Calculated interfacial tension of the copper-matte system at 1473 K.

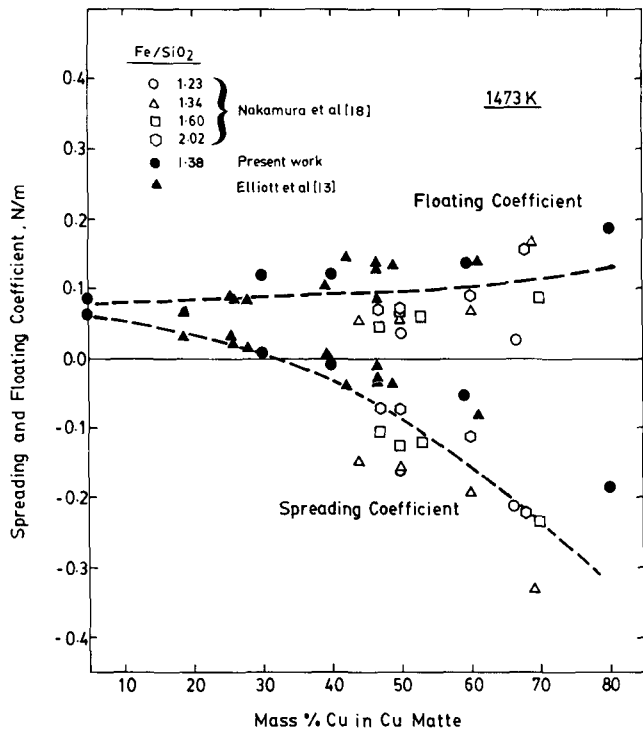


Fig. 11—Spreading and flotation coefficients of the matte-slag-gas system at 1473 K.

copper before and after the experiment were comparable. Samples 1 and 2 were analyzed for oxygen after the experiment using a LECO* high-temperature oxygen

*LECO is a trademark of LECO Corporation, St. Joseph, MO.

analyzer. The concentration of oxygen detected in these samples were 13 and 5 ppm, respectively. The high oxygen content in sample 1 was attributed to the presence of mullite particles attached to the bottom of the frozen copper drop which were observed under the scanning electron microscope. Sulfur analysis was performed on sample 4 and the amount detected was less than 1 ppm. Therefore, the concentrations of both oxygen and sulfur are too low to have any effect on the surface tension determined in this study. From all of the relevant supporting data presented, it is concluded that the copper surface tension data obtained in this study are accurate and reliable.

The effect of oxygen pressure on the surface tension of copper is presented in Figure 8 along with the results reported by Gallois and Lupis^[11] and Morita and Kasama.^[12] The surface tensions obtained are consistent with their data. All results show a decrease in copper surface tension with increase in the oxygen partial pressure.

Interfacial tensions of the matte-slag system measured in the present study are shown in Figure 9. The data are compared to those reported by Elliott and Mounier^[13] and Nakamura *et al.*^[18] Figure 9 shows that the results obtained from this study are in good agreement with the literature data. The data indicate a clear trend of increasing interfacial tension with increasing matte grade.

Using experimental conditions identical to those used

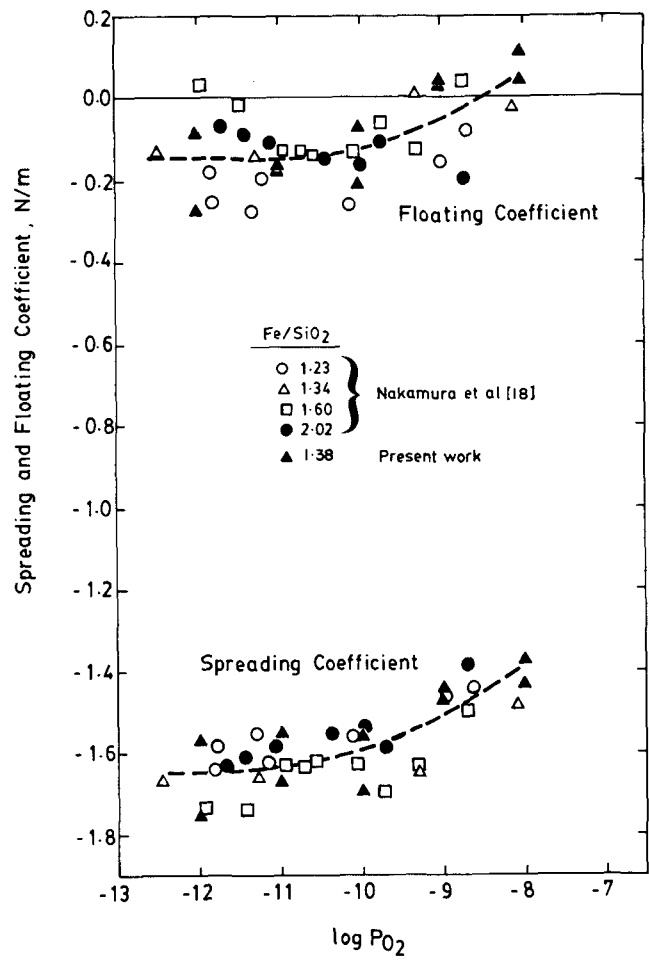


Fig. 12—Spreading and flotation coefficients of the copper-slag-gas system as a function of oxygen pressure at 1473 K.

for matte-slag experiments, the interfacial tension of copper in slag was measured and found to be 0.741 N/m. As expected, the value for copper is much higher than that for pure Cu_2S since the presence of sulfur in the copper drastically reduces the interfacial tension of the system. To facilitate the evaluation of the entrainment behavior in the copper-matte-gas and copper-slag-matte system, the interfacial tensions between copper and copper matte were calculated using the Girifalco-Good's equation (Eq. [10])^[14,15] together with Good's parameter of unity.^[14] The present results on the surface tension of copper, together with the data for copper mattes from Reference 16, were used in the calculation.

$$\gamma_{12} = \gamma_1 + \gamma_2 - 2\Phi(\gamma_1\gamma_2)^{1/2} \quad [10]$$

The calculated curve is shown in Figure 10. The results show a very slight dependency of interfacial tension on matte grade.

Combining the data presented in this study with those in the literature,^[13,16,17] the spreading and flotation coefficients of the matte-slag-gas, copper-slag-gas, copper-slag-matte, and copper-matte-gas systems were calculated. The ternary interfacial energy diagram for these systems was also constructed. For the purpose of these calculations, the surface tension of the fayalite slag was chosen to be 0.399 N/m.^[17] Due to the accumulation of

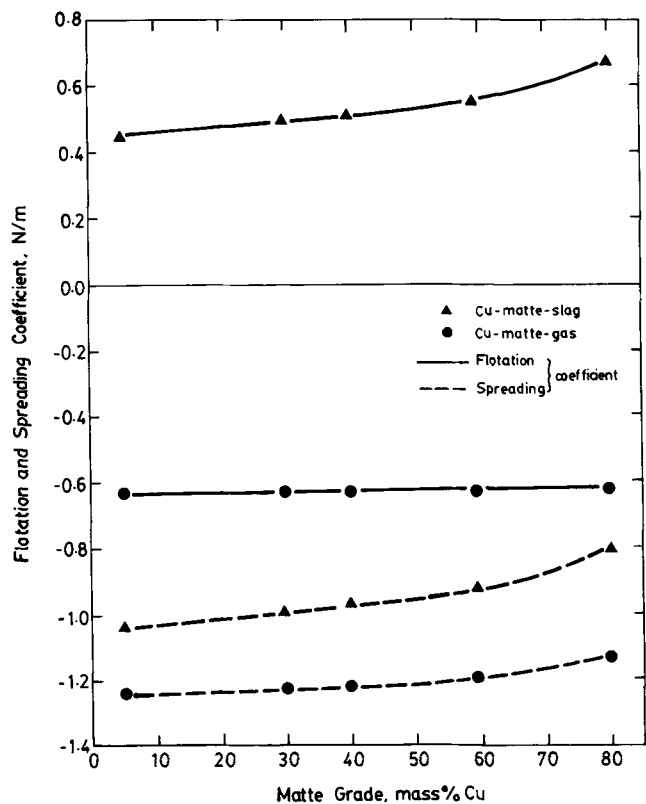


Fig. 13—Spreading and flotation coefficients of the copper-slag-matte and copper-matte-gas system at 1473 K.

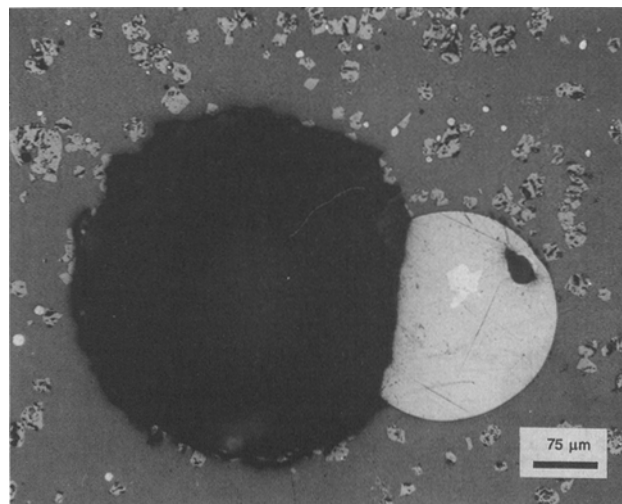


Fig. 15—Photomicrograph of a quenched commercial converter slag showing the attachment of a matte droplet to a gas bubble. Slag has an Fe/SiO₂ ratio of 1.40 and a nominal copper content of ~20 pct.

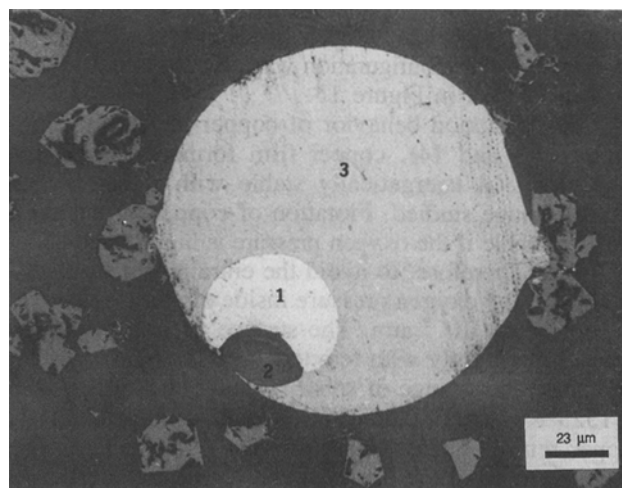


Fig. 16—Photomicrograph of a commercial converter slag showing the inclusion of a copper (1) and slag (2) drop inside a matte droplet (3). Composition of slag is the same as the sample shown in Fig. 15.

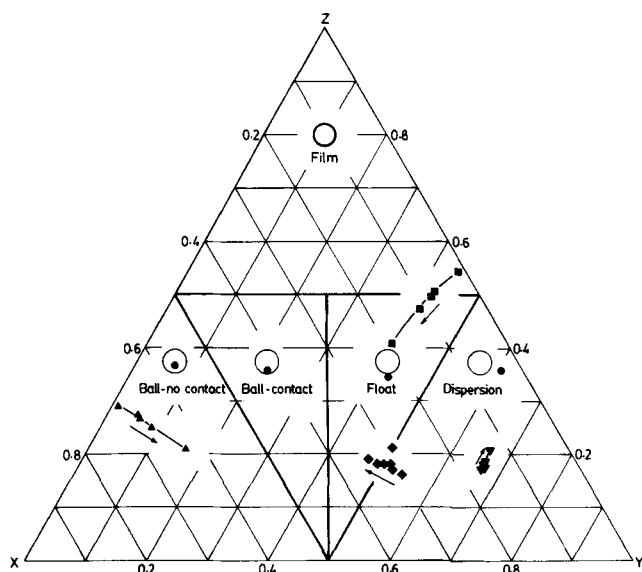


Fig. 14—Ternary interfacial energy diagram for the matte-slag-gas, copper-slag-gas, copper-matte-gas, and copper-slag-matte system at 1473 K. The direction of arrows indicates increasing matte grade or oxygen pressure. The different symbols represent the (■) matte-slag-gas, (◆) copper-slag-gas, (▼) copper-matte-gas, and (▲) copper-slag-matte systems.

uncertainties with each addition and subtraction, the estimated maximum standard deviation value associated with the spreading and flotation coefficients is 0.1 N/m.

The spreading and flotation coefficients and the ternary interfacial energy diagram of the four systems examined are given in Figures 11 through 14 together with literature data from various sources.^[13,18] For the matte-slag-gas system (Figures 11 and 14), the mattes showed a positive spreading coefficient at matte grades lower than about 32 mass pct Cu. On the other hand, the flotation coefficient is positive over the entire matte grade. Since both flotation and spreading are favored by a positive coefficient, matte film formation on gas bubbles is only possible at matte grades lower than about 32 mass pct Cu. However, the results indicate that flotation cannot be avoided by adjusting the matte composition. The same behavior is predicted by the ternary interfacial energy

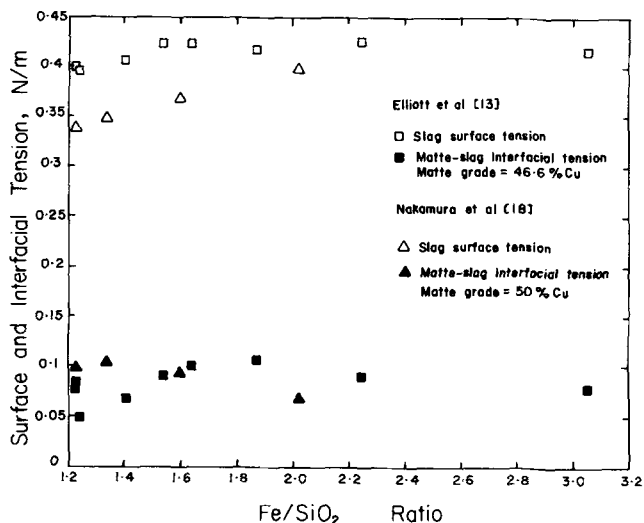


Fig. 17—Surface tension of fayalite slag and interfacial tension of copper-matte-slag system as a function of slag composition at 1473 K. Interfacial tension data obtained at constant matte grade.

diagram. This diagram also predicts that matte droplets will be floated by attaching themselves to the bottom of gas bubbles. This configuration was observed in quenched slags, as shown in Figure 15.

For the flotation behavior of copper in fayalite slags (Figures 12 and 14), copper film formation on rising bubbles is not energetically stable within the oxygen pressure range studied. Flotation of copper by gas bubbles is possible if the oxygen pressure is higher than about 10^{-9} atm. Therefore, to avoid the entrainment of metallic copper, the oxygen pressure inside the furnace should be kept below 10^{-9} atm. The surface tension of copper varies only slightly with temperature. Therefore, within the temperature range of smelting and converting (1423 to 1523 K), the flotation and spreading coefficients of copper remain negative and relatively unchanged. The observed trend of the flotation and spreading coefficient in Figure 12 is primarily caused by the surface tension behavior of copper in oxygen atmosphere.

Although copper drops may not be floated directly by gas bubbles, they may be carried upward by rising matte droplets attached to gas bubbles. When the copper-slag-matte system was examined (Figures 13 and 14), the results revealed that it is energetically feasible for copper drops to attach themselves to matte droplets and be floated by rising gas bubbles. Figure 14 indicates clearly that copper will penetrate the matte droplets as drop attachment occurs. This configuration was observed in a commercial slag and is shown in Figure 16. Although the calculated copper-matte interfacial tension values were based on Girifalco-Good's equation and may not be totally accurate, Figure 13 shows that a very large deviation from the calculated interfacial tension values is required in order to alter the observed behavior. Therefore, it can be concluded that copper may be floated by rising matte droplets of any composition. The spreading and flotation coefficients of the copper-matte-gas system were also determined and are shown in Figure 13. It was found that both coefficients were negative over the entire matte composition. Therefore, flotation of copper by gas

bubbles in the matte phase is not energetically feasible. A comparison of Figures 11 through 14 clearly indicates that the ternary interfacial energy diagram provides a more visual and easily perceptible representation of the flotation behavior of the entrained phases in the slag.

The effect of the change in the Fe/SiO₂ ratio of the slag on both the spreading and flotation coefficients is not significant, as shown in Figure 11. At the high copper content of the matte phase, the values of the spreading coefficient increase very slightly with increasing Fe/SiO₂ ratio. However, in the case of the flotation coefficients, the corresponding data showed no trends with change in Fe/SiO₂ ratio. For the copper-slag-gas system, the effect of the Fe/SiO₂ ratio of the slag on the spreading and flotation coefficients is also not significant, as shown in Figure 12, over a large P_{O_2} range. The small influence of Fe/SiO₂ ratio on both the spreading and flotation coefficients is attributed to the small change in slag surface tension and matte-slag interfacial tension over a large composition range. This is illustrated in Figure 17, which is plotted using data tabulated in References 13 and 18.

IV. CONCLUSIONS

The surface tension of copper was measured as a function of temperature. The results are consistent with literature data. The effect of oxygen on the surface tension of copper was investigated. It was found that oxygen partial pressure in the range of 10^{-12} to 10^{-8} atm has only a moderate effect in lowering the surface tension. The interfacial tension of the copper matte-fayalite slag system was measured. A nonlinear relationship was observed between the matte grade and the interfacial tension.

Using spreading and flotation coefficients as well as ternary interfacial energy diagrams, the flotation behavior of various entrained phases was examined. It was found that matte flotation in the slag phase by rising gas bubbles cannot be eliminated by altering the matte grade. Flotation of copper in the slag by gas bubbles can be avoided by maintaining the oxygen pressure below about 10^{-9} atmosphere. In the copper-slag-matte system, the flotation of copper by the rising matte droplets cannot be avoided by changing the matte composition. The results also indicated that the Fe/SiO₂ ratio of the slag only has a minor effect on droplet entrainment behavior.

ACKNOWLEDGEMENTS

This work was supported by the Natural Sciences and Engineering Research Council of Canada and the Energy, Mines and Resources, CANMET, Canada. We are grateful to Dr. T. Nakamura of Kyushu Institute of Technology, Kitakyushu, Japan, for his helpful comments and discussion.

REFERENCES

1. R. Minto and W.G. Davenport: *Trans. Inst. Min. Metall.*, 1972, vol. 81, pp. C59-C62.
2. W.D. Harkins: *The Physical Chemistry of Surface Films*, Reinhold, New York, NY, 1952.
3. D.S. Conochie and D.G.C. Robertson: in *Gas Injection into Liquid*

- Metals*, A.E. Wraith, ed., University of Newcastle upon Tyne, United Kingdom, 1979, pp. K1-K8.
4. T. Utigard and J.M. Toguri: *Metall. Trans. B*, 1985, vol. 16B, pp. 333-38.
 5. Y. Rotenberg, L. Boruvka, and A.W. Neumann: *J. Colloid Int. Sci.*, 1983, vol. 93, pp. 169-83.
 6. L.D. Lucas: *Mem. Sci. Rev. Metall.*, 1964, vol. 61, pp. 1-24.
 7. K. Ikeda, A. Tamura, Y. Shiraishi, and T. Saita: *Bull. Res. Inst. Miner. Dress. Metall., Tohoku Univ.*, 1973, vol. 29, pp. 24-36.
 8. G.H. Kaiura and J.M. Toguri: *Can. Metall. Q.*, 1979, vol. 18, pp. 155-64.
 9. D.A. Harrison, D. Yan, and S. Blairs: *J. Chem. Thermodyn.*, 1977, vol. 9, pp. 1111-19.
 10. S.M. Kaufman and T.J. Whalen: *Acta Metall.*, 1965, vol. 13, pp. 797-805.
 11. B. Gallois and C.H.P. Lupis: *Metall. Trans. B*, 1981, vol. 12B, pp. 549-57.
 12. Z. Morita and A. Kasama: *Trans. Jpn. Inst. Met.*, 1980, vol. 21, pp. 522-30.
 13. J.F. Elliott and M. Mounier: *Can. Metall. Q.*, 1982, vol. 21, pp. 415-28.
 14. T. Utigard and J.M. Toguri: *Metall. Trans. B*, 1987, vol. 18B, pp. 695-702.
 15. L.A. Girifalco and R.J. Good: *J. Phys. Chem.*, 1957, vol. 61, pp. 904-09.
 16. S. Tokumoto, A. Kasama, and Y. Fujioka: *Technol. Rep., Osaka Univ.*, 1982, vol. 22, pp. 453-63.
 17. T. Nakamura, F. Noguchi, Y. Ueda, and J.M. Toguri: Kyushu Institute of Technology, Kitakyushu, Japan, unpublished research, 1991.
 18. T. Nakamura, F. Noguchi, Y. Ueda, and S. Nakajyo: *J. Min. Metall. Inst. Japan*, 1988, vol. 104, pp. 531-36.